

2004-07-14

# Late Hercynian leucogranites modelling as deduced from new gravity data: The example of the Millevaches massif (Massif Central, France)

Gebelin, A

<http://hdl.handle.net/10026.1/11005>

---

10.2113/175.3.239

Bulletin de la Societe Geologique de France

---

*All content in PEARL is protected by copyright law. Author manuscripts are made available in accordance with publisher policies. Please cite only the published version using the details provided on the item record or document. In the absence of an open licence (e.g. Creative Commons), permissions for further reuse of content should be sought from the publisher or author.*

## **Late Hercynian leucogranites modelling as deduced from new gravity data : the example of the Millevaches massif (Massif Central, France)**

AUDE GEBELIN<sup>1</sup>, GUILLAUME MARTELET<sup>2</sup>, MAURICE BRUNEL<sup>1</sup>, MICHEL FAURE<sup>3</sup> and PHILIPPE ROSSI<sup>2</sup>

*Key words.* – Gravimetry, Density, Laccolith, Millevaches massif, Crustal structure.

*Abstract.* – The Millevaches granitic complex, located in the northern part of the French Massif Central, is elongated in a N-S direction, perpendicular to the main E-W trend of the Hercynian belt. It is affected on its limits and in its core by several ductile shear zones that have necessarily played a great role in the emplacement and exhumation of the massif. Based on gravity modelling and recent field observations, this study intends to highlight the massif structure at depth and discuss its mode of emplacement and relations with the surrounding terrains.

The new gravity and density measurements on the north-east part of the Millevaches massif improve the gravity coverage of the northern Limousin. Using these new data we model the deep structure of the Millevaches plateau. The density measurements made on the different types of granites of the massif, and on the surrounding terrains improve the interpretation of the Bouguer anomaly. Analysis and inversion of the residual Bouguer anomaly in the area show that the Millevaches massif is 2 to 4 km-thick, from north to south and from west to east, locally rooting down to about 6 km deep in its eastern and southern terminations. These two zones coincide with porphyritic plutons and, because of the complex composite structure of the massif, cannot be definitively interpreted as feeding zones. In the field, the N-S-oriented Pradines vertical fault affects the core of the massif on 4 to 5 km width. Microstructural observations evidence that the faulting is contemporaneous of the granites emplacement. We suggest that this tectonic lineament could have triggered the migration of the magma, although it is not related to a clear gravity anomaly. AMS measurements in the north-central part of the Millevaches massif suggest that the magnetic foliation and lineation display a general sub-horizontal pattern. Moreover, on the western border of the Millevaches massif, the Argentat deep seismic profile shows sub-horizontal layering of gneisses and micaschists and evidences normal faulting offset of this layering along Argentat fault. This agrees fairly well with the gravity results, suggesting that (i) the Millevaches massif would be at a high structural level in the crust, (ii) the exhumation of the massif would have been favoured along the Argentat normal fault. As a whole, the massif can be described as a laccolith, 2 to 4 km-thick, emplaced as a “magmatic lens” into the sub-horizontally foliated gneisses and micaschists.

### **Modélisation des leucogranites tardi-hercyniens à partir de nouvelles données gravimétriques : l'exemple du massif de Millevaches (Massif central)**

*Mots-clés.* – Gravimétrie, Densité, Laccolithe, Massif de Millevaches, Structure crustale.

*Résumé.* – Le massif granitique de Millevaches orienté N-S est transverse aux grands chevauchements de la chaîne hercynienne. Il est affecté en son cœur et au niveau de ses bordures par de grandes zones de cisaillement ductiles. On propose que ces accidents aient joué un rôle significatif dans la mise en place et dans les mécanismes d'exhumation du massif. Sur la base d'une modélisation gravimétrique et d'observations de terrain, cette étude est destinée à mieux comprendre la structure en profondeur du massif, son contexte de mise en place et ses relations avec l'encaissant.

Afin d'améliorer la couverture gravimétrique régionale, de nouvelles données gravimétriques ont été acquises sur la partie nord-est du Millevaches et permettent de modéliser la structure profonde du massif. En complément, des mesures de densité ont été effectuées sur l'ensemble des granites du plateau de Millevaches, ainsi que sur les formations encaissantes pour affiner la lecture de l'anomalie gravimétrique. L'observation de l'anomalie résiduelle et de son inversion, permettent de modéliser ce massif granitique comme un laccolithe dont le plancher se situe entre 2 et 4 km de profondeur du nord vers le sud et de l'ouest vers l'est. Deux zones d'épaississement bien marquées (épaisseur supérieure à 5 km) sont mises en évidence, à l'est, à l'aplomb du granite de Meymac et à l'extrémité sud du Millevaches. Elles sont toutes deux superposées au faciès porphyroïde et compte tenu de la structure complexe du massif elles ne peuvent être considérées avec certitude comme zones d'alimentation de l'ensemble du massif.

L'analyse microstructurale de la zone de cisaillement des Pradines parallèle à l'orientation N-S du massif et qui l'affecte au centre sur une largeur de 4 à 5 km, met en évidence des textures sub-solidus dans les granites qui indiquent une mise en place synchrone de ces derniers. Comme hypothèse de travail, nous proposons que cet accident décrochant représente une zone de faiblesse ayant joué un rôle dans la migration des magmas. Cette structure qui n'est que faiblement marquée en gravimétrie pourrait néanmoins avoir favorisé la migration des magmas.

<sup>1</sup> Laboratoire Dynamique de la Lithosphère, Université Montpellier II, CC060, Place E. Bataillon, 34095 Montpellier cedex 5.  
e-mail : gebelin@dstu.univ-montp2.fr

<sup>2</sup> BRGM, CDG-MA, BP 6009, 45060 Orléans cedex 2.

<sup>3</sup> Dept. des Sciences de la Terre, Université d'Orléans, 45060 Orléans cedex 2  
Manuscrit déposé le 24 avril 2003 ; accepté après révision le 9 janvier 2004.

L'acquisition de données d'anisotropie de susceptibilité magnétique effectuées dans la partie nord du massif de Millevaches mettent en évidence des directions préférentielles de fluidalité magmatique sub-horizontales.

En accord avec le modèle gravimétrique, ces résultats indiquent que les granites du Millevaches se seraient mis en place dans la foliation horizontale préexistante des gneiss et des micaschistes. Par ailleurs, le profil de sismique réflexion Argentat qui recoupe la bordure ouest du Millevaches indique une structuration en lames horizontales de l'encaissant formé par les gneiss et micaschistes. Il montre également une remontée de ces structures et du plancher du Millevaches à l'est de la faille d'Argentat démontrant le rôle important joué par celle-ci dans les mécanismes d'exhumation du massif.

## INTRODUCTION

The Variscan Massif Central, France, is known to be a collision belt which first experienced crustal stacking and thickening [Matte, 1986], followed by extension and thinning [Mattauer *et al.*, 1988 ; Faure, 1989 ; Van den Driessche and Brun, 1989 ; Faure *et al.*, 1990 ; Burg *et al.*, 1990 ; Faure, 1995]. Syn- or post-tectonic leucogranite plutons related to the post thickening thermal event crop out over large areas within the Massif Central hiding the earlier crustal structures. Some authors propose that leucogranites were emplaced during the Carboniferous post-collision crustal thinning episode [Faure, 1989 ; Faure and Pons, 1991]. Most Hercynian leucogranites are bounded by ductile shear zones which probably played a significant role in magma emplacement and/or subsequent exhumation of the massifs. Relationships between magmatism and deformation in orogenic belts are a large question. Indeed, close spatial and temporal relationships between faults and plutons have been recently described [Tikoff and St Blanquat, 1997]. Based on observation of geological maps several authors propose that magma ascent and emplacement is controlled by faults [Hutton, 1988 ; D'Lemos *et al.*, 1992]. Others show that magmatic processes can produce regional deformation [Tikoff *et al.*, 1999]. During their emplacement, large and hot magma volumes induce thermal heterogeneities that may disturb the regional deformation field. Shear zones can result from the instability propagation and in this case the pluton is closely related to their development [Holm, 1995]. The knowledge of depth processes is crucial for an overall understanding of phenomenon and requires using the geophysical tools. It is now well accepted that gravity modelling is appropriate to get a 3D image of geological bodies, and especially of granitic plutons [e.g. Vigneresse and Brun, 1983 ; Améglio, 1998 ; Martelet *et al.*, 1999]. The gravity modelling complements the structural study that is restricted to the surface interpretation compared to the inferred thickness of granitic plutons. In this study, the gravity modelling is performed using simple assumptions in order to bring a first overview of the Millevaches massif geometry at depth. Together with other structural and geophysical data, this brings new constraints to investigate the relationships between the massif and the host rocks as well as its mode of emplacement. This could be related to large ductile shear zones which affect the Millevaches massif on its boundaries and in its centre. Trying to detect a possible negative anomaly along the fault, evidence of close relationships between fault and magma, the gravity associated with the kinematics study will help us to understand the fault impact on the magmas emplacement and on the mechanism of exhumation. To infer the 3D shape

of several plutons in the Hercynian belt, several authors performed gravity modelling [Martelet *et al.*, 1999 ; Audrain *et al.*, 1989 ; Dumas *et al.*, 1990 ; Améglio *et al.*, 1994]. These studies allowed to raise questions in some cases about the bubble shape of plutons in orogenic belts. According to Vigneresse [1995] the granites emplaced during extensional deformation are thin with many root zones whereas the ones emplaced in context of shear deformation or compression are more deeply rooted with only one or a few roots. We will compare the Millevaches massif shape with others surrounding Hercynian plutons.

## GEOLOGICAL SETTING

This study focuses on the Millevaches granitic complex, located on the northwestern part of the Massif Central, France (fig. 1). The Millevaches massif is 160 km-long, it follows a N-S trend and is sub-perpendicular to the E-W to WNW-ESE main thrusts of the Hercynian belt. On its western side, the Millevaches plateau is separated from the Limousin metamorphic units [Floc'h, 1983] by the ductile and brittle Argentat fault ; to the north, it is separated from the Guéret granitic massif by the "St Michel de Veisse" dextral wrench fault, and in the east it is separated from cordierite anatexites and biotite-sillimanite paragneiss units by the Felletin - la Courtine shear zone, followed southward by the Ambrugeat fault (fig. 1). The massif is affected in its central part by the N-S Pradines ductile dextral wrench fault. Understanding the general kinematics of these major shear zones, their relations with plutonism and their role in the exhumation of the granitic massif is essential to better apprehend the transition between compressive, wrench and extensional tectonics in the Hercynian belt.

The Millevaches massif is composed of several porphyritic biotite granites and leucogranites plutons hosted in micaschists, forming N-S or NW-SE elongated stripes (fig. 1). Whole rock Rb/Sr isochrones give late Visean ages between 332 and 336 Ma [Augay, 1979 ; Monier, 1980] for the leucogranites emplacement. Furthermore,  $^{40}\text{Ar}/^{39}\text{Ar}$  step-heating age spectra performed on muscovites of leucogranites give ages between 335 and 337 Ma [Roig *et al.*, 2002]. According to Donnot [1965] the different magmas were emplaced at the same time. Other authors propose two generations of granites ; the porphyritic biotite granite resulting from melting of the lower crust are thought to be early compared to later leucogranites [Mouret, 1924 ; Raguin, 1938 ; Lameyre, 1966]. According to Monier [1980], the south of the Millevaches is composed of distinct plutons, each corresponding to a different melting event.

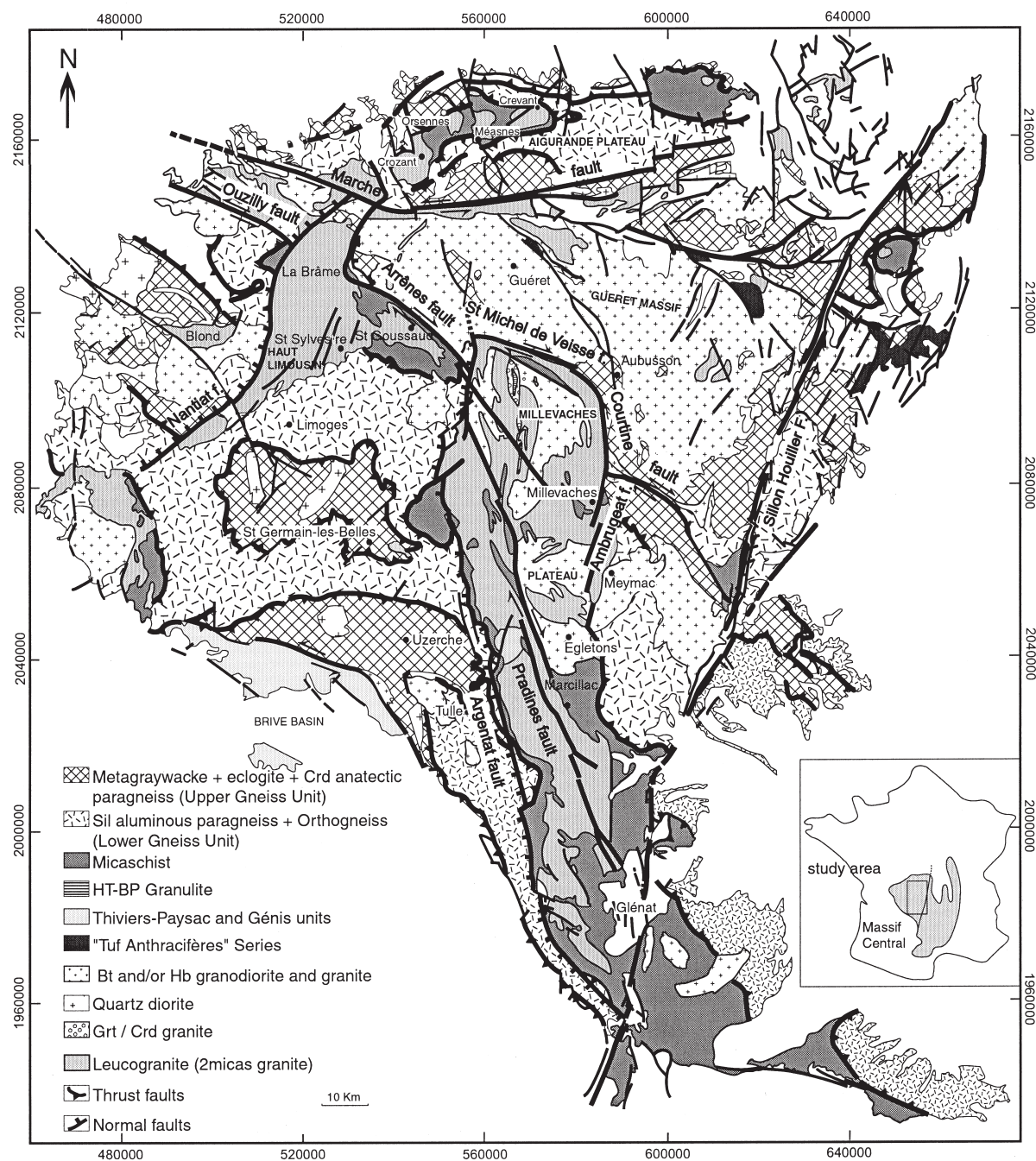


FIG. 1. – Simplified geological map of the northwestern part of the Massif Central, France.  
 FIG. 1. – Carte géologique simplifiée de la partie nord-ouest du Massif central.

In the northern part of the Millevaches, three main domains can be distinguished according to magnetic susceptibility anisotropy [Jover, 1986]. The earliest porphyritic biotite granites, related to cordierite-garnet granites, show N-S sub-horizontal magnetic lineation and vertical magnetic foliation planes, parallel to granulite lenses. These formations are cut by later leucogranites parted in two groups by the author [Jover, 1986]: the former having NW-SE vertical foliations and sub-horizontal lineations, the latter having E-W to NW-SE sub-horizontal lineations and foliations.

## GRAVITY DATA

### Data acquisition

In order to get sufficient gravity stations to model the deep structures of the Millevaches massif, we had to complete the regional gravity coverage. In addition to the data from the French Gravity Database (white dots on figure 2), we measured 200 new gravity stations in the northeastern part of the Millevaches massif (black dots on figure 2). In most parts of the 450 km<sup>2</sup> surveyed area, we sampled 0.5 km<sup>-2</sup>



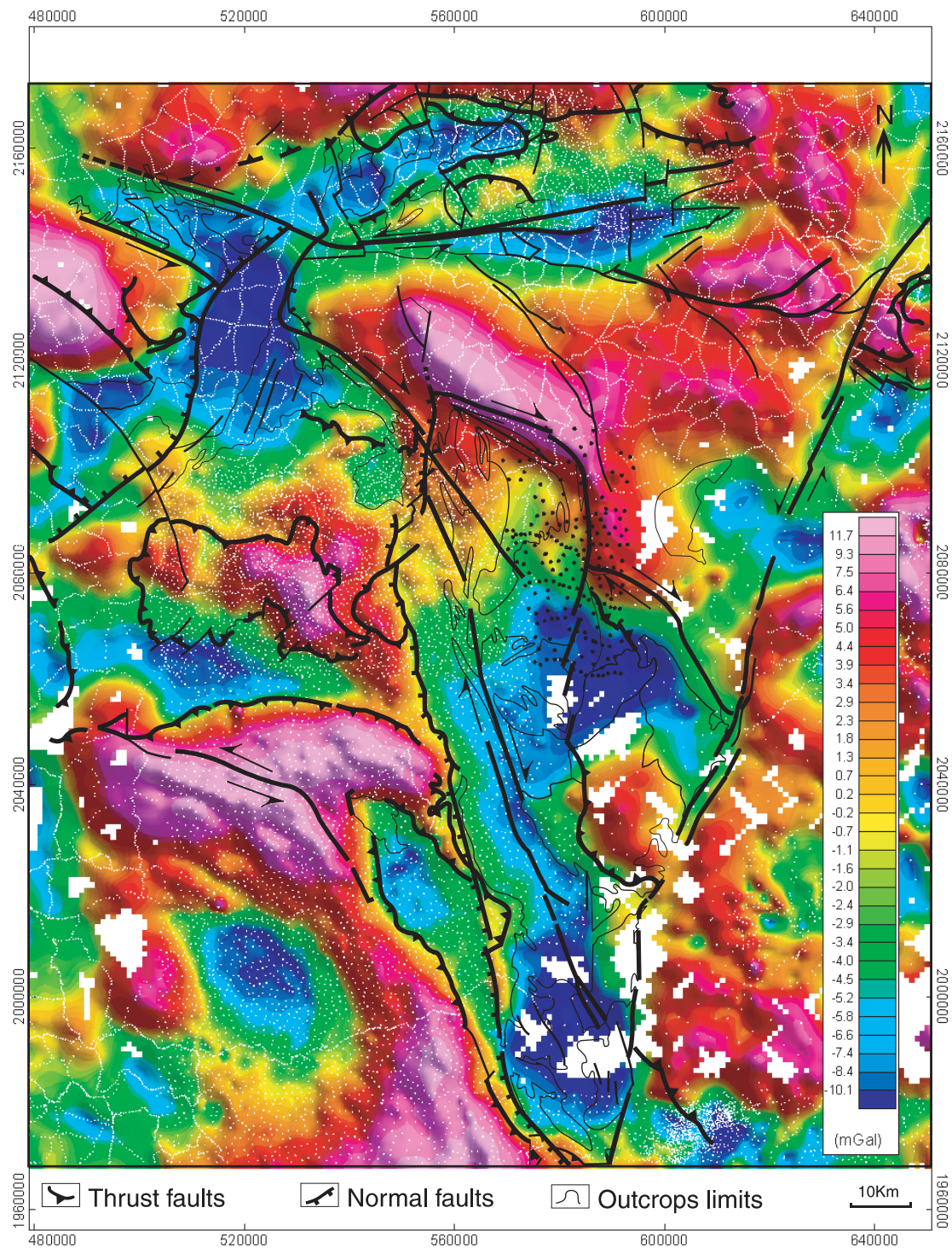


FIG. 2. – Residual Bouguer anomaly map of the northwestern part of the Massif Central. White dots correspond to the gravity coverage available in the French Gravity Database and black dots show the new gravity stations we measured.

FIG. 2. – Carte d'anomalie de Bouguer résiduelle de la partie nord-ouest du Massif central. Les points blancs et noirs localisent respectivement les données de la Banque gravimétrique française et les nouvelles stations gravimétriques mesurées dans cette étude.

gravity measurements. The data were measured with a Scintrex CG3-M micro-gravimeter which had been calibrated along the Sèvres-Orléans baseline. In the field, the measurements were tied to the CGF 65 French gravity base network. Stations were positioned with about 1 metre accuracy in altitude using bench marks from the Institut Géographique Na-

tional. Latitude and longitude were obtained using simple mode GPS positioning, with an accuracy of a few meters. The positioning was finally converted to the NTF French geodetic system using the WGS84 – Clarke 1880 transformation and projected into the Lambert II étendu projection, the altitude reference being at sea level.

## Data reduction and integration

The gravity anomaly was computed with respect to the theoretical value of  $g$  on Hayford-1930 ellipsoid. In order to obtain the complete Bouguer anomaly, we successively performed standard free air, plateau and terrain corrections. For the two latter, a  $2.6 \text{ g/cm}^3$  Bouguer reduction density was chosen, close to the expected density of the granites. Terrain corrections were computed up to 167 km to ensure a good consistency of the new dataset with the French Gravity Database [Martelet *et al.*, 2002]. Up to 53 m, terrain corrections were estimated in the field using Hammer charts [Hammer, 1939]. Beyond that distance, they were computed numerically using three DTM with grid sizes of 50 m, 250 m and 1 000 m, within annular zones of radius respectively 53 m-3 km, 3-10 km and 10-167 km. The error in the terrain correction is mostly due to the altitude offset between the DTM and the gravity stations : it varies from 0.1 to 0.6 mGal depending on the roughness of the topography. The mean quadratic error on the complete Bouguer anomaly due to the measurement, positioning and terrain corrections is 0.7 mGal.

## Residual Bouguer anomaly

In order to highlight the short wavelengths of the gravity map, we have computed a residual Bouguer anomaly map (fig. 2) by removing a degree 3 polynomial computed at the scale of the Massif Central and representing the regional trend. The resulting residual anomaly (fig. 2) (i) has apparently lost all regional trend, (ii) is consistent with the geology (negative anomalies are related to granites, and positive ones to gneissic units), (iii) fits fairly well with the outcropping limits of the Millevaches massif. Using the density measurements results (table I), the residual Bouguer anomaly map is consistent with the location of lithotectonic units : negative gravity anomalies are found to coincide with the granites (average density 2.62), whereas positive anomalies are related to the heavier gneissic or micaschists units (average density respectively 2.78 and 2.74). Hence, the Brême, St Sylvestre, and St Goussaud granitic complexes are related to clear negative anomalies which are persistent to the southwest and strengthen under the Blond leucogranite (NW of Limoges). To the north, the anomaly is divided into three branches. To the east and west, the negative anomaly underlines the leucogranites along the Marche fault. Finally, the negative anomaly heads to the northeast where, on the plateau of Aigurande, it clearly limits, from west to east, the leucogranitic plutons of Crozant, Orsennes, Measnes and Le Crevant, which are very well isolated as Dumas *et al.* [1990] suggested. Surprisingly, north of the Millevaches, the Guéret granite is underlined by an abnormal positive anomaly, which is comparable in intensity to that observed in the synforms of Uzerche or St Germain-Belles, west of the Millevaches (location on fig. 1). These are eclogite-bearing metagrauwackes of density about 2.83, much higher than the granites. The positive anomaly associated with the Guéret granite therefore indicates the limited thickness of the pluton and suggests that the massif is underlain by high density rocks. Indeed, cordierite anatexites crop out within a tectonic window in the northwestern part of the Guéret massif. This high density unit also plunges gently underneath the granite at its south-

ern limit, which suggests that it possibly underlies the overall massif.

With respect to its large extension, the Millevaches massif exhibits a relatively weak negative anomaly, suggesting a rather thin and laccolithic-like geometry. This is in agreement with the interpretation of the Argentat deep seismic profile which crosses the western border of the Millevaches plateau [Bitri *et al.*, 1999]. This profile shows the sub-horizontal structure of micaschists and the normal offset of the footwall of the fault which suggests an exhumation of the Millevaches plateau compared to the surrounding terrains. In this scheme the Argentat normal fault, located at the western border of the Millevaches plateau (fig. 1), would have played a major role in the exhumation of the massif [Ledru and Autran, 1987 ; Mattauer *et al.*, 1988 ; Faure, 1995 ; Roig *et al.*, 1998]. In the southern and eastern parts of the Millevaches, the negative anomaly strengthens, indicating thickening and the probable existence of two roots, which are found to be associated with porphyritic plutons. North of the massif, the negative anomaly decreases, suggesting northward thinning of the granite. Close to the Guéret granitic massif, the anomaly even becomes positive probably due to the presence of nearby high density cordierite anatexites that would underlie the Guéret massif. In order to give quantitative estimates of these interpretations, the variations in thickness of the Millevaches have been computed performing an inversion of the gravity field.

## GRAVITY INVERSION

The gravity field is inverted in terms of depth to the bottom of the granite using IBIS code [Chenot and Débeglia, 1990]. Prior to the inversion, the average depth of the modelled interface is calculated using Spector and Grant [1970] spectral analysis method. Then, assuming a density contrast of 0.11 (2.73-2.62) between the granite and the host rocks, the interface is iteratively deformed and its gravity effect compared to the Bouguer anomaly until the misfit between both is considered small. Figure 3 shows the geometry of the obtained granite/micaschists interface. Average thickness of the granite ranges between 2 and 4 km, with a maximum of about 6 km, which is in good agreement with estimations published on nearby massifs [e.g. Audrain *et al.*, 1989], or on massifs with comparable extension [e.g. Pétrequin, 1979 ; Talbot, 2003]. Uncertainties attached to the modelled geometry of the pluton floor are mainly related to the uncertainty on densities. We have chosen a constant density contrast between the granites and the surrounding rocks in order to keep the modelling as simple as possible. Indeed, we have considered neither depth-dependent densities, nor varying densities of the pluton basement, since we have poor constraints on these parameters. Moreover, in accordance with results obtained in comparable conditions for the Sidobre pluton [Améglio *et al.*, 1994], our tests show that uncertainties of 0.01 to 0.02  $\text{g/cm}^3$  on the density contrast used for the inversion shifts the average depth of the pluton floor by about 250 to 500 m, without significantly altering its shape. As previously suggested in the residual Bouguer anomaly map, the bottom of the massif is deeper in its eastern, and southern parts, with thickness reaching 5 to 6 km. In the south, this deep-rooting could be associated



TABLE I. – Density measurements.

Density measurements obtained by double weighing method with an average uncertainty on each sample of 0.01 g/cm<sup>3</sup>. Several calibrations using heavy liquids allowed to verify the accuracy of the density measurements.

TABL. I. – Mesures de densité.

Mesures de densité réalisées par la méthode de la double pesée, avec une incertitude moyenne de 0,01 g/cm<sup>3</sup> sur chaque échantillon. Plusieurs calibrages aux liqueurs denses ont permis de s'assurer de la justesse des densités établies par pesée.

N° Ech.	D (g/cm3)	Type lithologique	Localisation	N° Ech.	D (g/cm3)	Type lithologique	Localisation
D2	2,58	granite à 2 micas porphyroïde	Meymac	D66	2,67	granite à Bt porphyroïde	massif de Millevaches
D3	2,58	granite à 2 micas porphyroïde	Meymac	D67	2,72	aubussonite	Aubusson
D4	2,59	granite à 2 micas porphyroïde	Meymac	D68	2,65	leucogranite mylonitique	Felletin-La Courtine
D5	2,64	granite à 2 micas porphyroïde	Meymac	D69	2,61	granite à Bt type Guéret mylonitique	Felletin-La Courtine
D6	2,66	gneiss anatectique un peu altéré	Sornac	D70	2,66	granite type guéret	Felletin-La Courtine
D7	2,72	gneiss anatectique	Sornac	D71	2,71	aubussonite	Felletin-La Courtine
D8	2,7	gneiss anatectique	Sornac	P-I-C	2,64	leucogranite très frais	Peyrat-le-château
D9	2,6	aubussonite altérée	Sornac	C	2,64	leucogranite très frais	Compeix
D10	2,75	gneiss anatectique très frais	Sornac	D72	2,58	granite à 2 micas porphyroïde	Meymac
D11	2,62	leucogranite	massif de Millevaches	D73	2,6	granite	égletons
D12	2,6	leucogranite	massif de Millevaches	D74	2,62	granite	égletons
D13	2,6	leucogranite	massif de Millevaches	D75	2,62	leucogranite	massif de Millevaches
D14	2,59	granite à Bt porphyroïde	massif de Millevaches	D77	2,61	leucogranite	massif de Millevaches
D15	2,6	granite à Bt porphyroïde	massif de Millevaches	D78	2,64	leucogranite	massif de Millevaches
D16	2,65	granite à Bt porphyroïde	massif de Millevaches	D79	2,69	micaschiste	Est de Marcillac
D17	2,61	granite à Bt porphyroïde	massif de Millevaches	D80	2,7	micaschiste	Est de Marcillac
D18	2,61	leucogranite porphyroïde	massif de Millevaches	D81	2,62	gneiss oeilée	Est de Marcillac
D19	2,6	granite à Bt porphyroïde	massif de Millevaches	D82	2,66	gneiss anatectique	Est de Marcillac
D20	2,64	granite à Bt porphyroïde	massif de Millevaches	D83	2,7	gneiss anatectique	Est de Marcillac
D22	2,61	granite à Bt porphyroïde	massif de Millevaches	D84	2,75	gneiss anatectique très frais	Est de Marcillac
D23	2,63	Leucogranite à grain moyen	massif de Millevaches	G5	2,6	leucogranite	massif de Millevaches
D24	2,59	leucogranite porphyroïde	massif de Millevaches	G27	2,73	aubussonite	massif de Millevaches
D25	2,6	leucogranite à grain fin	massif de Millevaches	G40	2,59	leucogranite	massif de Millevaches
D26	2,65	microgranite	massif de Millevaches	G42	2,62	leucogranite	massif de Millevaches
D27	2,64	granite à Bt porphyroïde	massif de Millevaches	G52	2,62	leucogranite	massif de Millevaches
D28	2,61	leucogranite	Domsps	G61	2,63	leucogranite	massif de Millevaches
D29	2,76	gneiss anatectique	Sussac	G78	2,54	granite à Bt	massif de Millevaches
D31	2,61	aubussonite altérée	Châteauneuf-la-Forêt	G91	2,63	leucogranite	massif de Millevaches
D32	2,65	gneiss anatectique	Châteauneuf-la-Forêt	G174	2,64	granite à Bt	massif de Millevaches
D33	2,72	aubussonite très fraîche	vers Bujaleuf	3	2,61	leucogranite mylonitique	bordure Est du Millevaches
D34	2,64	granite mylonitique	vers Bujaleuf	5	2,62	leucogranite mylonitique	bordure Est du Millevaches
D35	2,6	granite à Bt porphyroïde	NW de Peyrat-le-Château	14	2,72	gneiss anatectique	bordure Est du Millevaches
D36	2,64	granite à Bt	NW de Peyrat-le-Château	25	2,66	gneiss anatectique	bordure Est du Millevaches
D37	2,6	leucogranite porphyroïde	NW de Peyrat-le-Château	47	2,72	aubussonite	bordure Est du Millevaches
D38	2,6	leucogranite	NW de Peyrat-le-Château	71a	2,62	granite guéret cataclaté	bordure Est du Millevaches
D39	2,6	gneiss anatectique altéré	NW de Peyrat-le-Château	95	2,68	ultramylonite granite guéret	bordure Est du Millevaches
D40	2,61	microgranite	NW de Peyrat-le-Château	96	2,71	ultramylonite granite guéret	bordure Est du Millevaches
D41	2,65	gneiss anatectique	NW de Peyrat-le-Château	98b	2,64	leucogranite mylonitique	bordure Est du Millevaches
D42	2,97	gabbro/ dolérite	NW de Peyrat-le-Château	103	2,66	granite guéret protomylonitique	bordure Est du Millevaches
D43	2,63	leucogranite mylonitique	NW de Peyrat-le-Château	104	2,74	granite guéret protomylonitique	bordure Est du Millevaches
D44	2,76	micaschiste frais	Châtelus-le-Marcheix	105	2,66	granite guéret protomylonitique	bordure Est du Millevaches
D45	2,65	leucogranite	St Goussaud	113	2,76	granite guéret protomylonitique	bordure Est du Millevaches
D46	2,61	leucogranite	St Goussaud	119	2,67	granite guéret protomylonitique	bordure Est du Millevaches
D47	2,67	microgranite faciès Guéret	W de Guéret	126	2,6	leucogranite mylonitique	bordure Est du Millevaches
D48	2,64	granite à Bt type Guéret	W de Guéret	157	2,7	gneiss bt/sil	bordure Est du Millevaches
D49	2,67	aubussonite altérée	W de Guéret	180	2,64	Granite de Guéret mylonitique	bordure Est du Millevaches
D50	2,64	gneiss à bt/sil	Dun-le-Palestel	189	2,62	leucogranite mylonitique	bordure Est du Millevaches
D51	2,7	gneiss anatectique	Celle Dunoise	198c	2,72	gneiss anatectique frais	bordure Est du Millevaches
D52	2,71	gneiss anatectique	Celle Dunoise	198d	2,78	gneiss anatectique très frais	bordure Est du Millevaches
D53	2,7	gneiss anatectique	Celle Dunoise	225b	2,62	leucogranite mylonitique	bordure Est du Millevaches
D54	2,66	gneiss anatectique	Celle Dunoise	227	2,62	leucogranite mylonitique	bordure Est du Millevaches
D55	2,67	granite à Bt type Guéret	W de Guéret	236	2,64	leucogranite mylonitique	bordure Est du Millevaches
D56	2,57	granite à Bt type Guéret	W de Guéret	238	2,59	leucogranite mylonitique	bordure Est du Millevaches
D57	2,66	granite à Bt type Guéret	NW de Bourgneuf	245	2,67	granite	bordure Est du Millevaches
D58	2,61	leucogranite mylonitique	massif de Millevaches	253	2,61	granite type guéret	bordure Est du Millevaches
D59	2,64	granite à Bt porphyroïde	massif de Millevaches	265	2,63	leucogranite mylonitique	bordure Est du Millevaches
D60	2,62	leucogranite	massif de Millevaches	279	2,59	granite	bordure Est du Millevaches
D61	2,66	granite à Bt porphyroïde	massif de Millevaches	283	2,64	leucogranite mylonitique	sud de Dun-le-Palestel
D62	2,7	granite à Bt porphyroïde	massif de Millevaches	284	2,64	leucogranite mylonitique	sud de Dun-le-Palestel
D63	2,62	leucogranite	massif de Millevaches	345	2,72	micaschiste	gorges du Chavanon
D64	2,62	granite à Bt porphyroïde	massif de Millevaches	346	2,71	gneiss anatectique	gorges du Chavanon
D65	2,64	granite à Bt porphyroïde	massif de Millevaches	349b	2,81	micaschiste très frais	gorges du Chavanon

with the Glénat porphyritic granite rather than with the shallow leucogranites that mark out the Argentat fault (Roig, personal communication). Related to the easternmost negative anomaly, mining work in the Meymac area revealed the occurrence of a buried late granite [Burnol *et al.*, 1980]. It is however difficult to know whether the anomaly is due to the Meymac porphyroid granite or to the late

leucogranite body. Figure 4 presents a geological cross-section (profile A A') through the Millevaches granitic massif.

In the central part of the massif strongly affected by the Pradines shear zone, the gravity does not detect any large anomaly. The N-S oriented Pradines fault affects leucogranites and porphyritic biotite granites of the Millevaches massif in a 4 to 5 km-wide corridor. The N-S

trending vertical foliation and sub-horizontal lineation define a consistent pattern associated with the emplacement of granites during dextral shearing. Indeed, from south to

north within the shear zone, the leucogranites are typical biotite-muscovite C-S orthogneisses, and mylonites that indicate a dextral sense of shear (fig. 5). Furthermore, the microstructural study of Pradines dextral wrench fault mylonites shows sub-solidus deformation textures (fig. 6) : rectangular grain boundaries shape form a reticular or mosaic-like pattern indicating extensive grain boundary migration, typical of high temperature sub-solidus deformation [Gapais *et al.*, 1986 ; Tommasi and Vauchez., 1994]. These observations suggest a synchronous emplacement of leucogranites with the Pradines fault activity. Vertically foliated gneiss xenoliths prolongate the Pradines fault to the north. This occurrence advocates that the fault could have locally weakened the crust and favoured the migration of magmas.

Eastward and close to the leucogranite mylonites, the porphyritic biotite granites show magmatic textures with a N-S to NNW-SSE preferential orientations of the (010) plane in K-feldspars which become NW-SE south-eastwards [Mezure, 1980]. According to field relationships at the regional scale [Lameyre, 1966] the porphyritic biotite granite could have been emplaced at the same time as the leucogranites or more likely just before. We propose that the trend of this NW-SE foliation recorded strain field during the Pradines fault activity. In this last case the magma should not crystallise everywhere to record the effects of the dextral wrench Pradines fault.

## DISCUSSION

Following Améglio *et al.* [1997] gravity and structural results for several plutons show that magma emplacement is largely controlled by the anisotropy and rheology of the

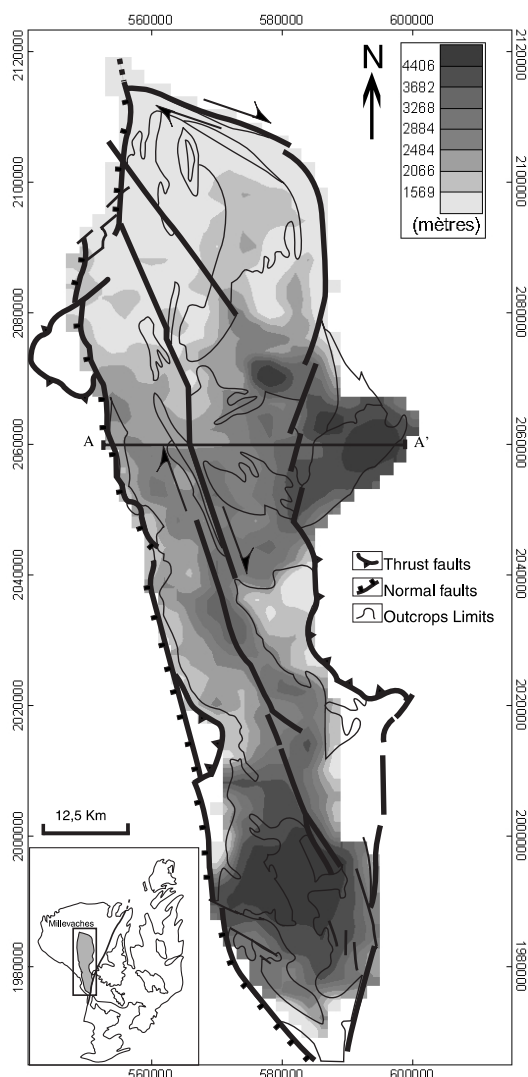


FIG. 3. – Map of the depth to the granite/micaschists interface, obtained by inversion of the gravity anomaly using the IBIS code. A A' : Cross-section, fig. 4.

FIG. 3. – Carte de profondeur de l'interface granite/encaissant obtenue par inversion de l'anomalie gravimétrique à l'aide du logiciel IBIS. A A' : coupe de la figure 4.

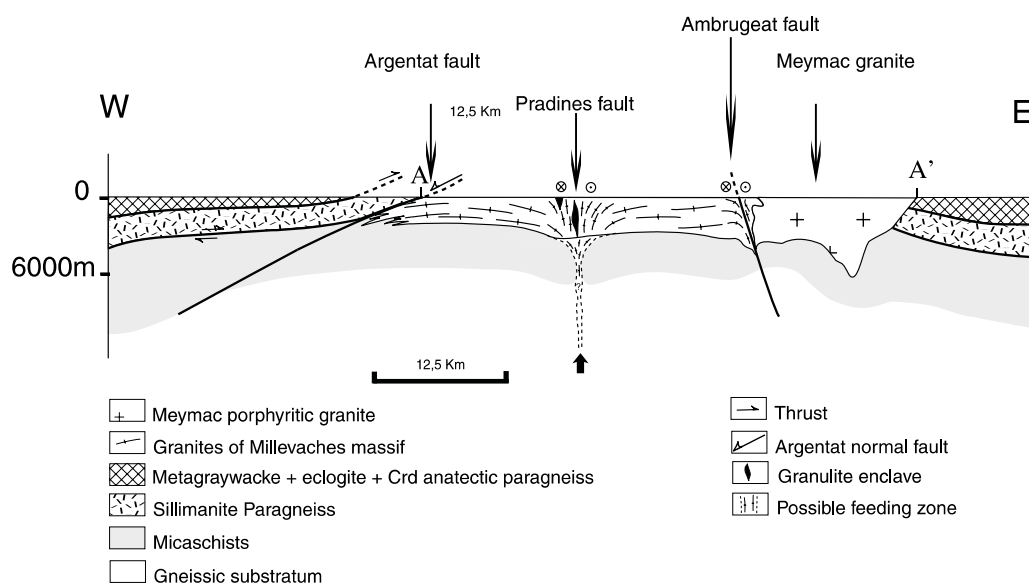


FIG. 4. – Sketch geological cross-section. (see location on fig. 3).

FIG. 4. – Coupe géologique schématique interprétative. (Voir la localisation sur la figure 3).



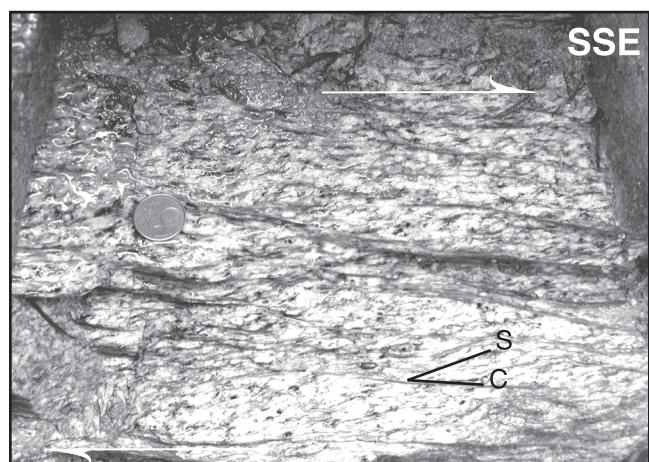


FIG. 5. – Typical C-S structures developed in the leucogranites of the Pradines fault indicating a dextral sense of shearing.

FIG. 5. – Structures C-S affectant les leucogranites de la faille des Pradines indiquant un sens de cisaillement dextre.

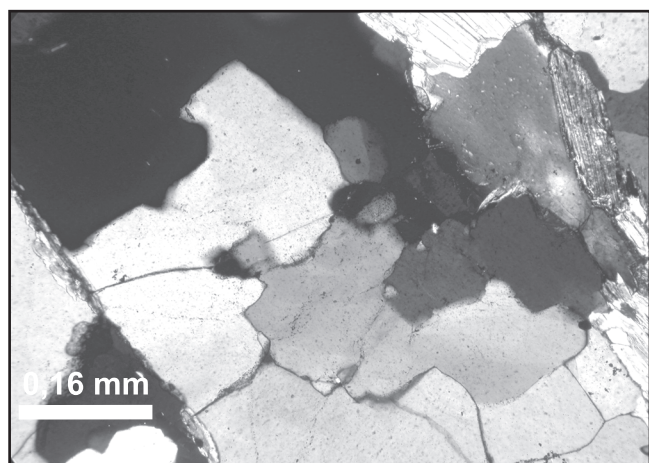


FIG. 6. – Quartz microstructures within foliated granite showing rectangular contours forming a reticular or mosaic-like pattern typical of high temperature deformation.

FIG. 6. – Microstructures du quartz montrant des contours rectangulaires qui forment un réseau réticulaire ou en mosaïque typique d'une déformation de haute température.

crust, in particular around the brittle-ductile transition. Local dilatancy of the brittle crust may be achieved under either compressive or extensive regime, but dominated by transcurent movements. These authors differentiate “flat-shaped” and “wedge-shaped” plutons on geometrical criteria and related tectonic regime criteria : (i) flat-shaped plutons have much broader horizontal than vertical extension and would spread parallel to the pre-existing tectonic layering of the crust, whereas, (ii) wedge-shaped plutons would infill more or less vertical fractures in the brittle crust. In addition, relations between plutons and the tectonic structures is generally evidenced ; whether these relations are genetic or related to the exhumation is often less clear. This is illustrated in the Limousin area, where several plutonic complexes were emplaced during the late-Hercynian period. The leucogranitic complex of la Brême – St Sylvestre dated at  $318 \pm 5$  Ma and  $324 \pm 4$  Ma by U-Pb method [Holliger *et al.*, 1986] has a flat-shaped ge-

ometry, with a rather low thickness of about 2 km [Audrain *et al.*, 1989], and an overall flat foliation. Likewise, the Sidobre granite located in the Montagne Noire (SW Massif central) was emplaced at  $304 \pm 8$  Ma [Pin, 1991], and appears as a 2 to 3 km thick sill, the emplacement of which was favoured by normal faults that also certainly played a role of feeding zone [Améglio *et al.*, 1994]. On the opposite, the plutons of the Aigurande plateau are rather of the wedge-shaped type. The Crevant leucogranitic massif is dated at  $312 \pm 6$  Ma [Petitpierre and Duthou, 1980] by Rb/Sr on whole rock and Crozant and Orsennes at  $312 \pm 20$  Ma [Rolin *et al.*, 1982] by the same method. The bodies are rooted southward around 3 km depth and spread laterally [Dumas *et al.*, 1990]. Owing to their close relationships, their emplacement is certainly linked with the Marche senestral wrench fault. These plutons could be compared with those of the South Armorican Shear Zone, such as the Mortagne pluton [Guineberteau *et al.*, 1987], which was emplaced between 300 and 360 Ma [Hanmer *et al.*, 1982 ; Le Corre *et al.*, 1991], deeply rooted into the shear zone and extrusive beyond the surface toward NE.

The Millevaches massif is the largest one. It was emplaced during the same late Hercynian period. Our model shows a large and rather thin batholith that can be classified in the “flat-shaped” type. In the context of the Hercynian orogeny, a wealth of geological considerations, synthesised by Faure and Pons [1991] document the emplacement of such type of plutons in a late-orogenic extensional tectonic environment.

Other tabular Hercynian granites have been recognized in western Europe and NW Africa. The idea of magma injection through fault and lateral expansion has already been discussed by Lagarde *et al.* [1990] about the late Carboniferous plutons of the Moroccan Meseta. To explain the emplacement of granitic plutons within high structural levels along crustal faults and their tabular shape, he suggests that faults collect melts at depth and control sites of emplacement within shallow crustal levels in which rheology permit the lateral expansion of magma [Lagarde *et al.*, 1990]. Similarly, the Itaporanga pluton in the northeast of Brazil is an example of granite that emplaced into a shear zone and spread out laterally as a sill [Archanjo *et al.*, 1999]. According to Hutton [1996], the Itaporanga pluton presents a syntectonic emplacement because of the magmatic and magnetic fabrics which are coherent with the country rock deformation. Relationships between faulting and granitic ascent have also been described in the Himalayas with emplacement of leucogranites along the North Himalayan Detachment [Burg and Brunel, 1984 ; Searle, 2003]. This fault zone behaves like a barrier to the magma ascent and controls the pluton emplacement in an extensional shear zone [Guillot *et al.*, 1995].

Owing to its overall tabular shape and geometric relationship with the surrounding terrains, the emplacement of the Millevaches massif can apparently be explained by this process : once it has reached the upper crust, the magma spreads laterally into the sub horizontal micaschist foliation (profile AA', figure 4). Lately, its exhumation is favoured along several faults that bound its limits and especially the Argentat normal fault. In the present state of knowledge, as a working hypothesis, we propose to interpret the Millevaches as a laccolitic intrusion driven and emplaced above a N-S trending vertical lineament.

However, the question of the magma feeding process still needs investigations since only a weak negative anomaly is expressed along the N-S Pradines shear zone. According to Fyfe [1973], or Reches and Fink [1988], we imagine the magma conduits as very narrow, jagged and instable pipes that disappear at the end of the magma transfer and give in consequence a weak anomaly.

## CONCLUSION

During the Hercynian orogeny large amounts of magmas resulting from the partial melting of the pre-Variscan basement [Cuney *et al.*, 1990] were produced, as can presently be observed in the Limousin area (Massif central, France). The process of magma segregation, their ascent and emplacement mechanisms, as well as their relationships with the regional tectonics are still debated. Gravity modelling combined with structural analysis yield a first overview of the Millevaches massif geometry at depth. Together with other structural and geophysical data, this brings new constraints that help investigate the relationships between the massif and the host rocks, as well as its mode of emplacement.

New gravity and rock densities have been measured which improve the gravity knowledge of the northern Limousin. Analysis and inversion of the residual Bouguer anomaly in the area show that the Millevaches massif is 2 to 4 km-thick, from north to south, rooting down to about 6 km depth in its eastern and southern terminations. These two zones coincide with porphyritic plutons but, because of the complex composite structure of the massif, cannot be definitively interpreted as feeding zones for the whole massif. Independent AMS and seismic results are in good agreement with the overall flat-lying geometry we derive from gravity modelling. These geophysical constraints also sug-

gest, in agreement with field observations, that the exhumation of the massif was achieved along several boundary faults and especially the Argentat normal fault. The scenario of emplacement of the massif as a laccolith at a high crustal level and its exhumation in relation with tectonic structures seems compatible with previously recognised situation for other batholiths in the late-Hercynian extensional context.

We further suggest that the Pradines shear zone, which is oriented parallel to the massif length and affects its core on a 4 to 5 km-wide corridor, could have triggered the migration of the magma (profile AA', figure 4). However, the question of the magma feeding process requires further investigations, since only a weak negative anomaly is expressed along the N-S Pradines fault. In the field, throughout the shear corridor in the leucogranites along the Pradines fault, typical C-S structures indicating a dextral sense of shear have been confirmed. Moreover, in this zone, quartz microstructures showing rectangular contours forming a mosaic-like pattern are typical of high temperature sub-solidus deformation coeval with leucogranite cooling.

Combining new geochronology ( $^{40}\text{Ar}/^{39}\text{Ar}$  method on the Pradines shear zones, together with the U-Pb method to determine the crystallization age of leucogranites), microstructural and ASM data, will be essential to further understand the internal magmatic processes, as well as the geodynamic context of the Millevaches massif emplacement.

*Acknowledgments.* – We thank J.-Y. Roig and C. Truffert for fruitful discussions. We are grateful to M. Diamant for providing us with a microgravimeter, and N. Debégliat for initiating us to the IBIS inversion software. We thank M. Jézequel for facilitating the density measurements. We used Geosoft software for the geophysical data mapping. This work is a contribution to research program entitled "Massif Central/ Limousin" of the Service de la Carte Géologique de la France, funded by BRGM.

## References

- AMEGLIO L. (1998). – Gravimétrie et forme tridimensionnelle des plutons granitiques. – Thèse de Doctorat, Univ. Toulouse III, 245 p.
- AMEGLIO L., VIGNERESSE J.-L. & BOUCHEZ J.-L. (1997). – Granite pluton geometry and emplacement mode inferred from combined fabric and gravity data. In : J.-L. BOUCHEZ, D.H.W. HUTTON & W.E. STEPHENS, Eds., *Granite : from segregation of melt to emplacement fabrics*. – Kluwer Academic Publishers, Dordrecht, 199-214.
- AMEGLIO L., VIGNERESSE J.-L., DARROZES J. & BOUCHEZ J.-L. (1994). – Forme du massif granitique du Sidobre (Montagne Noire, France) : sensibilité de l'inversion des données gravimétriques au contraste de densité. – *C. R. Acad. Sci.*, Paris, **319**, 2, 1183-1190.
- ARCHANJO C.-J., DA SILVA, E.-R. & CABY R. (1999). – Magnetic fabric and pluton emplacement in a transpressive shear zone system : the Itaporango porphyritic granitic pluton (northeast Brazil). – *Tectonophysics*, **312**, 331-345.
- AUDRAIN J., VIGNERESSE J.-L., CUNNEY M. & FRIEDRICH M. (1989). – Modèle gravimétrique et mise en place du complexe hyperalumineux de Saint-Sylvestre (Massif central français). – *C. R. Acad. Sci.*, Paris, **309**, 1907-1914.
- AUGAY J.-F. (1979). – Les leucogranites et monzogranites de la région d'Eymoutiers-Peyrat le Château (massif du Millevaches, Massif central français). Gisement et pétrologie. – Unpubl. doctoral Dissertation, University of Lyon I, Lyon.
- BITRI A., TRUFFERT C., BELLOT J.-P., BOUCHOT V., LEDRU P., MILESI J.-P. & ROIG J.-Y. (1999). – Imagerie des paléochamps hydrothermaux As-Au-Sb d'échelle crustale et des pièges associés dans la chaîne varisque : sismique réflexion verticale (GéoFrance3D : Massif central français). – *C. R. Acad. Sci.*, Paris, **329**, 771-777.
- BURG J.-P., BRUN J.-P. & VAN DEN DRIESSCHE J. (1990). – Le sillon houiller du Massif central français : faille de transfert pendant l'amincissement crustal de la chaîne varisque ? – *C. R. Acad. Sci.*, Paris, **311**, II, 147-152.
- BURG J.-P., BRUNEL M., GAPAIS D., CHEN G.M. & LIU G.H. (1984). – Deformation of leucogranites of the crystalline Main Central Sheet in southern Tibet (China). – *J. Struct. Geol.*, **6**, 5, 535-542.
- BURNOL L., PERONNE Y. & VAUCORBEIL H. (1980). – La coupole cachée de leucogranite de Neuf-Jours (Corrèze) et les minéralisations en tungstène associées. – *Chron. Rech. Min.*, **455**, 93-116.
- CHENOT D. & DEBEGLIAT N. (1990). – Three-dimensional gravity or magnetic constrained depth inversion with lateral and vertical variation of contrast. – *Geophysics*, **55**, 327-335.
- CUNNEY M., FRIEDRICH M., BLUMENFELD P., BOURGUIGNON A., BOIRON M.-C., VIGNERESSE J.-L. & POTY B. (1990). – Metallogensis in the French part of the Variscan orogen. Part I : U preconcentrations in pre-Variscan and Variscan formations ; a comparison with Sn, W and Au. – *Tectonophysics*, **177**, 39-57.
- D'LEMOIS R.S., BROWN M. & STRACHAN R.A. (1992). – Granite magma generation, ascent and emplacement within a transpressional orogen. – *J. Geol. Soc. London*, **149**, 487-496.



- DONNOT M. (1965). – Micaschistes et granites du plateau de Millevaches. – *Ann. Fac. Sci.*, Univ. Clermont-Ferrand, **27**, 139 p.
- DUMAS E., FAURE M. & PONS J. (1990). – L'architecture des plutons leucogranitiques du plateau d'Aigurande et l'amincissement crustal tardi-varisque. – *C. R. Acad. Sci.*, Paris, **310**, Série II, 1533-1539.
- FAURE M. (1989). – L'amincissement crustal de la chaîne varisque à partir de la déformation ductile des leucogranites du Limousin. – *C. R. Acad. Sci.*, Paris II, **309**, 1839-1845.
- FAURE M. (1995). – Late Carboniferous extension in the Variscan French Massif Central. – *Tectonics*, **14**, 132-153.
- FAURE M. & PONS J. (1991). – Crustal thinning recorded by the shape of the Namurian-Westphalian leucogranite in the Variscan belt of the northwest Massif Central, France. – *Geology*, **19**, 730-733.
- FAURE M., PROST A. & LASNE E. (1990). – Déformation ductile extensive d'âge namuro-westphalien dans le plateau d'Aigurande, Massif central français. – *Bull. Soc. géol. Fr.*, **8**, 189-197.
- FLOCH J.-P. (1983). – La série métamorphique du Limousin central : une traverse de la branche ligérienne de l'orogène varisque, de l'Aquitaine à la zone broyée d'Argentat (Massif central français). – Thèse d'Etat, Univ. Limoges, 445 p.
- FYFE W.S. (1973). – The generation of batholiths. – *Tectonophysics*, **17**, 273.
- GAPAIS D. & BARBARIN B. (1986). – Quartz fabric transition in a cooling syntectonic granite (Hermitage massif, France). – *Tectonophysics*, **125**, 4, 357-370.
- GUILLLOT S., PECHER A. & LE FORT P. (1995). – Contrôles tectoniques et thermiques de la mise en place des leucogranites himalayens. – *C. R. Acad. Sci.*, Paris, **320**, 55-61.
- GUINEBERTEAU B., BOUCHEZ J.-L. & VIGNERESSE J.-L. (1987). – The Mortagne granite pluton (France) emplaced by pull-apart along a shear zone : structural and gravimetric arguments and regional implication. – *Geol. Soc. Amer. Bull.*, **99**, 763-770.
- HAMMER S. (1939). – Terrain corrections for gravimeter stations. – *Geophysics*, **4**, 184-194.
- HANMER S.K., LE CORRE C. & BERTHE D. (1982). – The role of Hercynian granites in the deformation and metamorphism of Brioverian and Paleozoic rocks of central Brittany. – *J. Geol. Soc. London*, **139**, 85-93.
- HOLLIGER P., CUNNEY M., FRIEDRICH M. & TURPIN L. (1986). – Age carbonifère de l'unité de Brême du complexe granitique peralumineux de St Sylvestre (NW du Massif central) défini par les données isotopiques U-Pb sur zircon et monazite. – *C. R. Acad. Sci.*, II, **303**, 1309-1314.
- HOLM D.K. (1995). – Relation of deformation and multiple intrusion in the Death Valley extended region, California, with implications for magma entrapment mechanism. – *J. Geophys. Res.*, **100**, 10495-10505.
- HUTTON D.H.W. (1988). – Granite emplacement mechanisms and tectonic controls : inferences from deformation studies. – *Trans. R. Soc. Edin.*, *Earth Sci.*, **79**, 245-255.
- HUTTON D.H.W. (1996). – The 'space problem' in the emplacement of granite. – *Episodes*, **19**, 114-119.
- JOVER O. (1986). – Les massifs granitiques de Guéret et du nord-Millevaches. Analyse structurale et modèle de mise en place (Massif central français). – Thèse, Univ. Nantes, 233 p.
- LAGARDE J.-L., BRUN J.-P. & GAPAIS D. (1990). – Formation des plutons granitiques par injection et expansion latérale dans leur site de mise en place : une alternative au diapirisme en domaine épizonal. – *C. R. Acad. Sci.*, Paris, **310**, 1109-1114.
- LAMEYRE J. (1966). – Leucogranites et muscovitisation dans le Massif central français. – Thèse, Univ. de Clermont-Ferrand, 264 p.
- LE CORRE C., AUVRAY B., BALLEVRE M. & ROBARDET M. (1991). – Le Massif armoricain. – *Sciences Géologiques*, **44**, 31-103.
- LEDRU P. & AUTRAN A. (1987). – L'édification de la chaîne Varisque dans le Limousin. Rôle de la faille d'Argentat à la limite Limousin-Millevaches. – *Prog. G.P.F., Doc. BRGM*, Orléans, 87-106.
- MARTELET G., DIAMENT M. & TRUFFERT C. (1999). – Un levé gravimétrique détaillé dans les Cévennes : apport à l'imagerie crustale (programme GéoFrance3D - Massif central). – *C. R. Acad. Sci.*, Paris, **328**, 727-732.
- MARTELET G., DEBEGLIA N. & TRUFFERT C. (2002). – Homogénéisation et validation des corrections de terrain gravimétriques jusqu'à la distance de 167 km sur l'ensemble de la France. – *C. R. Geosciences*, **334**, 449-454.
- MATTAUER M., BRUNEL M. & MATTE P. (1988). – Failles normales ductiles et grands chevauchements. Une nouvelle analogie entre l'Himalaya et la chaîne hercynienne du Massif central français. – *C. R. Acad. Sci.*, Paris II, **306**, 671-676.
- MATTE P. (1986). – Tectonics and plate tectonics model for the Variscan belt of Europe. – *Tectonophysics*, **126**, 329-374.
- MEZURE J.-F. (1980). – Etude structurale des granites d'Egletons, Meymac et Ussel (Nord). Contribution à l'estimation quantitative de la déformation. Pétrographie et géochimie. – Thesis of speciality, Univ. Clermont-Ferrand, 191p.
- MONIER G. (1980). – Pétrologie des granitoïdes du Sud Millevaches (Massif central français). Minéralogie, géochimie, géochronologie. – Thèse 3<sup>ème</sup> Cycle, Univ. Clermont II, 288p.
- MOURET G. (1924). – Sur la structure de la région granitique de Millevaches. – *C. R. Acad. Sci.*, Paris, **179**, 1612-1615.
- PETITPIERRE E. & DUTHOU J.-L. (1980). – Age westphalien par la méthode Rb/Sr du leucogranite de Crevant, Plateau d'Aigurande (Massif central français). – *C. R. Acad. Sci.*, **291**, 163-166.
- PETREQUIN M. (1979). – Etude gravimétrique du massif de la Margeride et de sa bordure méridionale. – Thèse 3<sup>ème</sup> cycle, Univ. Montpellier, 128p.
- PIN C. (1991). – Sr-Nd isotopic study of igneous and metasedimentary enclaves in some Hercynian granitoids from the Massif Central, France. In : J. DIDIER & B. BARBARIN, Ed., *Enclaves and granite petrology. – Developments in Petrology*, Elsevier, 333-343.
- RAGUIN E. (1938). – Contribution à l'étude du plateau de Millevaches (révision de la feuille de Limoges). – *Bull. Serv. Carte géol. Fr.*, **39**, **197**, 113-119.
- RECHES Z. & FINK J. (1988). – The mechanism of intrusion of the Inyo dike, Long Valley, California. – *J. Geophys. Res.*, **93**, 627-662.
- ROIG J.-Y., FAURE M. & TRUFFERT C. (1998). – Folding and granite emplacement inferred from structural, strain, TEM, and gravimetric analyses : The case study of the Tulle antiform, SW French Massif Central. – *J. Struct. Geol.*, **20**, 9-10, 1169-1189.
- ROIG J.-Y., FAURE M. & MALUSKI H. (2002). – Surimposed tectonic and hydrothermal events during the late-orogenic extension in the western French Massif Central : a structural and <sup>40</sup>Ar/<sup>39</sup>Ar study. – *Terra Nova*, **14**, 25-32.
- ROLIN P., DUTHOU J.-L. & QUENARDEL J.-M. (1982). – Datation Rb/Sr des leucogranites de Crozant et d'Orsennes : conséquences sur l'âge de la dernière phase de tectonique tangentielle du Plateau d'Aigurande (NW du Massif central français). – *C. R. Acad. Sci.*, II, **294**, 799-802.
- SEARLE M.P., SIMPSON R.L., LAW R.D., PARRISH R.R. & WATERS D.J. (2003). – The structural geometry, metamorphic and magmatic evolution of the Everest Massif, High Himalaya of Nepal-South Tibet. – *J. Geol. Soc. London*, **160**, 3, 345-366.
- SPECTOR A. & GRANT F.-S. (1970). – Statistical models for interpreting aeromagnetic data. – *Geophysics*, **35**, 293-302.
- TALBOT J.-Y. (2003). – Apport des études ASM et gravimétriques des plutons cévenols à la caractérisation structurale de l'évolution tardihercynienne du Massif central – Thèse de Doctorat, Université d'Orléans, 288 p.
- TIKOFF B. & SAINT BLANQUAT (de) M. (1997). – Transpressional shearing and strike-slip partitioning in the late Cretaceous Sierra Nevada magmatic arc, California. – *Tectonics*, **16**, 442-459.
- TIKOFF B., SAINT BLANQUAT (DE) M. & TEYSSIER C. (1999). – Translation and the resolution of the pluton space problem. – *J. Struct. Geol.*, **21**, 1109-1117.
- TOMMASI A. & VAUCHEZ A. (1994). – Magma-assisted strain localization in an orogen-parallel transcurent shear zone of southern Brazil. – *Tectonics*, **13**, 2, 421-437.
- VAN DEN DRIESCHE J. & BRUN J.-P. (1989). – Un modèle de l'extension paléozoïque supérieur dans le sud du Massif central. – *C. R. Acad. Sci.*, Paris, II, **309**, 1607-1613.
- VIGNERESSE J.-L. (1995). – Control of granite emplacement by regional deformation. – *Tectonophysics*, **249**, 173-186.
- VIGNERESSE J.-L. & BRUN J.-P. (1983). – Les leucogranites armoricains marqueurs de la déformation régionale : apport de la gravimétrie. – *Bull. Soc. géol. Fr.*, **XXV**, 3, 357-366.